PHYSICAL REVIEW B **79**, 020501(R) (2009)

Theory of Andreev reflection in junctions with iron-based high-T_c superconductors

Jacob Linder and Asle Sudbø
Department of Physics, Norwegian University of Science and Technology, N-7491 Trondheim, Norway
(Received 3 October 2008; published 7 January 2009)

We construct a theory for low-energy quantum transport in normal|superconductor junctions involving the recently discovered iron-based high-T_c superconductors. We properly take into account both Andreev bound surface states and the complex Fermi-surface topology in our approach and investigate the signatures of the possible order-parameter symmetries for the FeAs lattice. Our results could be helpful in determining the symmetry of the superconducting state in the iron-pnicitide superconductors.

DOI: 10.1103/PhysRevB.79.020501 PACS number(s): 74.20.Rp, 74.50.+r, 74.70.Dd

I. INTRODUCTION

Very recently, a family of iron-based superconductors with high transition temperatures was discovered with a concomitant avalanche of both experimental and theoretical activities.[1–12] The highest T_c measured so far in this class of materials is 55 K, and many experimental reports indicate signatures of unconventional superconducting pairing. However, it remains to be clarified what the exact symmetry is for both the orbital and spin parts of the Cooper pair wave function—there has, for instance, been reports of both nodal[11] and fully gapped[10] order parameters (OPs) in the literature up to now.

Probing the low-energy quantum transport properties of superconducting materials has proven itself as a highly useful tool to access information about the symmetry of the superconducting OP.[13] The conductance spectra of normal|superconductor (N|S) junctions often contain important and clear signatures of the orbital structure of the OP. For instance, when the OP contains nodes in the tunneling direction with a sign change across the nodes on each side of the Fermi surface, the conductance will display a large zero-bias conductance peak (ZBCP) due to the presence of Andreev surface bound states.[14]

Two recent studies[10,11] utilized the method of point-contact spectroscopy in order to study the symmetry of the superconducting OP in $LaFeAsO_{0.9}F_{0.1-\delta}$ and $SmFeAsO_{0.85}F_{0.15}$, respectively. The findings were in stark contrast. Namely, the large ZBCP found in $LaFeAsO_{0.9}F_{0.1-\delta}$ gave evidence of a nodal order parameter, while the data of $SmFeAsO_{0.85}F_{0.15}$ clearly indicated a nodeless OP. In both these studies, the Blonder-Tinkham-Klapwijk[15] (BTK) framework was used to analyze the data theoretically using the extension to anisotropic pairing by Tanaka and Kashiwaya.[16] In this model, one considers a cylindrical or spherical Fermi surface with a free-electron dispersion relation, which does not account for the nontrivial multiband Fermi-surface topology and dispersion relation in the iron pnicitides. One might argue that the extended BTK model nevertheless may suffice to describe the transport properties of these materials qualitatively, but this statement clearly warrants a detailed investigation.

In this Rapid Communication, we construct a theory of low-energy quantum transport properties of the iron-based high-T_c superconductors by considering a N|S junction relevant for point-contact spectroscopy and scanning-tunneling-microscopy measurements. In doing so, we model fairly accurately the Fermi-surface topology and the associated quasiparticle dispersions in order to see how this affects the results as compared with the usual BTK paradigm. We consider several possible OP symmetries which may be realized in the iron pnicitides. We organize this work as follows. In Sec. II, we introduce the theoretical framework which is used to obtain the tunneling conductance. In Sec. III, we present our main results and a discussion of these. Finally, we summarize in Sec. IV.

II. THEORY

We adopt the minimal two-band model derived in Ref. 8 [Fig. 1(a)], in which the normal-state Hamiltonian reads

$$H_N = \sum_{\mathbf{k}\sigma} \phi^\dagger_{\mathbf{k}\sigma} \begin{pmatrix} \epsilon_{\mathbf{k}x} - \mu & \epsilon_{\mathbf{k}xy} \\ \epsilon_{\mathbf{k}xy} & \epsilon_{\mathbf{k}y} - \mu \end{pmatrix} \phi_{\mathbf{k}\sigma}, \tag{1}$$

where the fermion basis $\phi_{\mathbf{k}\sigma}=[d_{\mathbf{k}x\sigma}, d_{\mathbf{k}y\sigma}]^T$ contains the annihilation operators for electrons in the d_{xz} and d_{yz} orbitals with spin σ and wave vector $\mathbf{k}$, respectively. We have also defined $\epsilon_{\mathbf{k}x}=-2t_1c_x-2t_2c_y-4t_3c_xc_y$, $\epsilon_{\mathbf{k}xy}=-4t_4s_xs_y$, and $\epsilon_{\mathbf{k}y}=-2t_2c_x-2t_1c_y-4t_3c_xc_y$, with $c_j=\cos(k_ja)$, $s_j=\sin(k_ja)$, $j=x,y$, and a the lattice constant. By diagonalizing the above Hamiltonian, one obtains

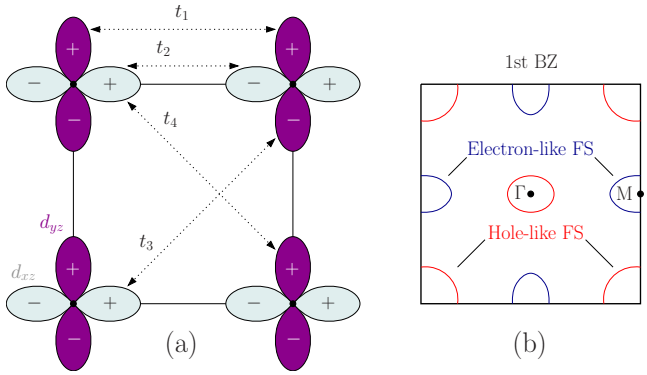

FIG. 1. (Color online) (a) Illustration of the two-dimensional FeAs plane with the d_{xz} and d_{yz} orbitals and hopping between them, as proposed in Ref. 8. (b) Sketch of the Fermi-surface topology for the long-lived quasiparticle excitations in a minimal two-band model (see main text for parameter values).

$$H_N = \sum_{\mathbf{k}\sigma} \tilde{\phi}^\dagger_{\mathbf{k}\sigma} \mathrm{diag}\{\Omega^+_{\mathbf{k}}, \Omega^-_{\mathbf{k}}\} \tilde{\phi}_{\mathbf{k}\sigma},$$

$$\Omega^\pm_{\mathbf{k}} = (\epsilon_{\mathbf{k}x} + \epsilon_{\mathbf{k}y})/2 - \mu \pm \sqrt{(\epsilon_{\mathbf{k}x} - \epsilon_{\mathbf{k}y})^2/4 + \epsilon^2_{\mathbf{k}xy}}, \quad (2)$$

where the new basis $\tilde{\phi}_{\mathbf{k}\sigma} = [\gamma^+_{\mathbf{k}\sigma}, \gamma^-_{\mathbf{k}\sigma}]^T$ consists of new fermion quasiparticle operators in the bands + and − which are hybrids of the d_{xz} and d_{yz} orbitals. The Fermi-surface topology is given by $\Omega^\pm_{\mathbf{k}} = 0$ and gives an electronlike band (+) and holelike band (−) shown in Fig. 1(b) for the choice $t_1 = -1$, $t_2 = 1.3$, $t_3 = t_4 = -0.85$, and $\mu = 1.54$, all measured in units of $|t_1|$. Our choice of parameter set is motivated by the fact that it reproduces the same Fermi-surface structure as the local-density approximation (LDA) band-structure calculations,[17] and it was also employed in Refs. 18 and 19. The new fermion operators are related to the old basis $\phi_{\mathbf{k}\sigma}$ by

$$\zeta_{\mathbf{k}} = \epsilon_{\mathbf{k}xy} / [(\epsilon_{\mathbf{k}x} - \epsilon_{\mathbf{k}y})/2 + \sqrt{(\epsilon_{\mathbf{k}x} - \epsilon_{\mathbf{k}y})^2/4 + \epsilon^2_{\mathbf{k}xy}}],$$

$$\phi^\dagger_{\mathbf{k}\sigma} P_{\mathbf{k}} = \tilde{\phi}^\dagger_{\mathbf{k}\sigma}, \quad P_{\mathbf{k}} = (1 + \zeta^2_{\mathbf{k}})^{-1/2} \times \begin{pmatrix} 1 & -\zeta_{\mathbf{k}} \\ \zeta_{\mathbf{k}} & 1 \end{pmatrix}. \quad (3)$$

We now introduce a superconducting pairing between the long-lived quasiparticles $\gamma^\lambda_{\mathbf{k}\sigma}$, with $\lambda = \pm$, which then automatically accounts for both interband and intraband pairings in the original fermion basis $\phi_{\mathbf{k}}$,

$$H_{\mathrm{SC}} = \sum_{\mathbf{k}\lambda} [\Delta^\lambda_{\mathbf{k}} (\gamma^\lambda_{\mathbf{k}\uparrow})^\dagger (\gamma^\lambda_{-\mathbf{k}\downarrow})^\dagger + \mathrm{H.c.}]. \quad (4)$$

In this way, we may diagonalize the total Hamiltonian $H = H_N + H_{\mathrm{SC}}$ by introducing a final fermion basis $\eta^\lambda_{\mathbf{k}} = [c^\lambda_{\mathbf{k}\uparrow}, c^\lambda_{-\mathbf{k}\downarrow}]^T$ describing the quasiparticle excitations in the superconducting state. After discarding unimportant constants, we find that

$$H = \sum_{\mathbf{k}\sigma\lambda} \sigma E^\lambda_{\mathbf{k}} (c^\lambda_{\mathbf{k}\sigma})^\dagger c^\lambda_{\mathbf{k}\sigma}, \quad E^\lambda_{\mathbf{k}} = [(\Omega^\lambda_{\mathbf{k}})^2 + |\Delta^\lambda_{\mathbf{k}}|^2]^{1/2}. \quad (5)$$

This result is formally identical to a two-band superconductor with gaps $\Delta^\lambda_{\mathbf{k}}$ and normal-state dispersions $\Omega^\lambda_{\mathbf{k}}$, with $\lambda = \pm$. The belonging wave functions which describe the quasiparticle excitations read

$$\Psi^\lambda_{\mathbf{k}} = \{[u^\lambda_{\mathbf{k}}, v^\lambda_{\mathbf{k}} e^{-i\phi^\lambda_{\mathbf{k}}}]^T e^{i\lambda \mathbf{k}^\lambda \cdot \mathbf{r}}, [v^\lambda_{\mathbf{k}} e^{i\phi^\lambda_{\mathbf{k}}}, u^\lambda_{\mathbf{k}}]^T e^{-i\lambda \mathbf{k}^\lambda \cdot \mathbf{r}}\},$$

$$(u^\lambda_{\mathbf{k}})^2 = 1 - (v^\lambda_{\mathbf{k}})^2 = \frac{1}{2}(1 + \sqrt{E^2 - |\Delta^\lambda_{\mathbf{k}}|^2}/E), \quad (6)$$

for quasiparticles with positive excitation energies $E \geq 0$. Here, $\mathbf{k}^\lambda$ denotes the Fermi momentum for band λ while $e^{i\phi^\lambda_{\mathbf{k}}} = \Delta^\lambda_{\mathbf{k}} / |\Delta^\lambda_{\mathbf{k}}|$.

We have now effectively described the superconducting state as a two-band model with gaps $\Delta^\pm_{\mathbf{k}}$ and normal-state dispersions $\Omega^\pm_{\mathbf{k}}$. This has allowed us to obtain a simple form for the wave functions in Eq. (6) that are to be used in the scattering problem below. The trade off for this advantage, however, is that the $\mathbf{k}$ dependence of the gap functions $\Delta^\pm_{\mathbf{k}}$ in general will become quite complicated. To see this, we may transform Eq. (4) back to the original fermion basis $\phi_{\mathbf{k}}$ by means of our expression for $P_{\mathbf{k}}$ in Eq. (3) to find that

$$H_{\mathrm{SC}} = \sum_{\mathbf{k}} [\Delta_{\mathbf{k}x} d^\dagger_{\mathbf{k}x\uparrow} d^\dagger_{-\mathbf{k}x\downarrow} + \Delta_{\mathbf{k}y} d^\dagger_{\mathbf{k}y\uparrow} d^\dagger_{-\mathbf{k}y\downarrow} + \Delta_{\mathbf{k}xy} (d^\dagger_{\mathbf{k}x\uparrow} d^\dagger_{-\mathbf{k}y\downarrow} - d^\dagger_{\mathbf{k}y\uparrow} d^\dagger_{-\mathbf{k}x\downarrow}) + \mathrm{H.c.}], \quad (7)$$

where $\Delta_{\mathbf{k}x}$ and $\Delta_{\mathbf{k}y}$ are the intraorbital gaps while $\Delta_{\mathbf{k}xy}$ is the interorbital gap. They are defined as

$$\Delta_{\mathbf{k}x} = (\Delta^+_{\mathbf{k}} + \zeta^2_{\mathbf{k}} \Delta^-_{\mathbf{k}})/\nu^+_{\mathbf{k}}, \quad \Delta_{\mathbf{k}y} = (\Delta^-_{\mathbf{k}} + \zeta^2_{\mathbf{k}} \Delta^+_{\mathbf{k}})/\nu^+_{\mathbf{k}},$$

$$\Delta_{\mathbf{k}xy} = \zeta_{\mathbf{k}} (\Delta^+_{\mathbf{k}} - \Delta^-_{\mathbf{k}})/\nu^+_{\mathbf{k}}, \quad \nu^\pm_{\mathbf{k}} = (1 \pm \zeta^2_{\mathbf{k}}). \quad (8)$$

We see that the interorbital pairing vanishes in the case where $\Delta^+_{\mathbf{k}} = \Delta^-_{\mathbf{k}}$. However, we emphasize that our model accounts for interorbital pairing $\Delta_{\mathbf{k}xy}$ in the original fermion basis and that $\Delta_{\mathbf{k}xy} \neq 0$ whenever $\Delta^+_{\mathbf{k}} \neq \Delta^-_{\mathbf{k}}$. We do not consider any interband pairing in the new diagonalized fermion basis. Assuming spin-singlet and even-frequency pairing, there are three possible s-wave symmetries $\{\Delta_0, \Delta_0(c_x + c_y), \Delta_0 c_x c_y\}$ and two possible d-wave symmetries $\{\Delta_0(c_x - c_y), \Delta_0 s_x s_y\}$ for the superconducting order parameters $\Delta_{\mathbf{k}x}$ and $\Delta_{\mathbf{k}y}$ in terms of the square lattice harmonics. The gaps in the $\pm$ quasiparticle hybridized bands are then obtained as $\Delta^+_{\mathbf{k}} = (\Delta_{\mathbf{k}x} - \zeta^2_{\mathbf{k}} \Delta_{\mathbf{k}y})/\nu^-_{\mathbf{k}}$ and $\Delta^-_{\mathbf{k}} = (\Delta_{\mathbf{k}y} - \zeta^2_{\mathbf{k}} \Delta_{\mathbf{k}x})/\nu^-_{\mathbf{k}}$. Note that the extended s-wave symmetry $\sim c_x c_y$ changes sign on the electron and hole Fermi surfaces, similar to the $s_\pm$ scenario suggested in Refs. 5 and 19.

III. RESULTS AND DISCUSSION

We are now in a position to evaluate the conductance of the system. The presence of a Fermi-vector mismatch between the normal and superconducting sides of the junction is assumed to be manifested through an effective decrease in the junction transmission. Since the Fermi velocity may be different in the two bands with normal-state dispersions $\Omega^\pm_{\mathbf{k}}$, we allow different barrier parameters $Z^\pm$ in the two bands. For a specified pairing symmetry, there are then four fitting parameters present: the barrier strength Z^λ and gap magnitude Δ^λ_0 for band $\lambda = \pm$. By generalizing the results of Refs. 15 and 16 to a two-band model which also takes into account the nontrivial Fermi-surface topology in Fig. 1(a), we obtain the following expression for the normalized tunneling conductance: $G(eV)/G_0 = \Sigma_{\lambda,k_y} f(k_y) \sigma^\lambda_S(eV) / [2 f(k_y) \sigma^\lambda_N]$, where $\sigma^\lambda_N = [1 + (Z^\lambda)^2]^{-1}$ and

$$\sigma^\lambda_S(eV) = \{\sigma^\lambda_N [1 + \sigma^\lambda_N |\Gamma^\lambda_+(\mathbf{k}, eV)|^2 + (\sigma^\lambda_N - 1) \times |\Gamma^\lambda_+(\mathbf{k}, eV) \Gamma^\lambda_-(\mathbf{k}, eV)|^2]\} / [|1 + (\sigma^\lambda_N - 1) \times \Gamma^\lambda_+(\mathbf{k}, eV) \Gamma^\lambda_-(\mathbf{k}, eV) \rho^\lambda(\mathbf{k})|^2],$$

$$\Gamma^\lambda_\pm(\mathbf{k}, eV) = \frac{eV - \sqrt{(eV)^2 - |\Delta(\pm\lambda k_x, k_y)|^2}}{|\Delta^\lambda(\pm\lambda k_x, k_y)|},$$

$$\rho^\lambda(\mathbf{k}) = \frac{\Delta^\lambda(-\lambda k_x, k_y)[\Delta^\lambda(\lambda k_x, k_y)]^*}{|\Delta^\lambda(-\lambda k_x, k_y) \Delta^\lambda(\lambda k_x, k_y)|}, \quad (9)$$

where $f(k_y) = \cos(k_y a/2)$ is a weighting function that models the directional dependence of the incoming quasiparticles.

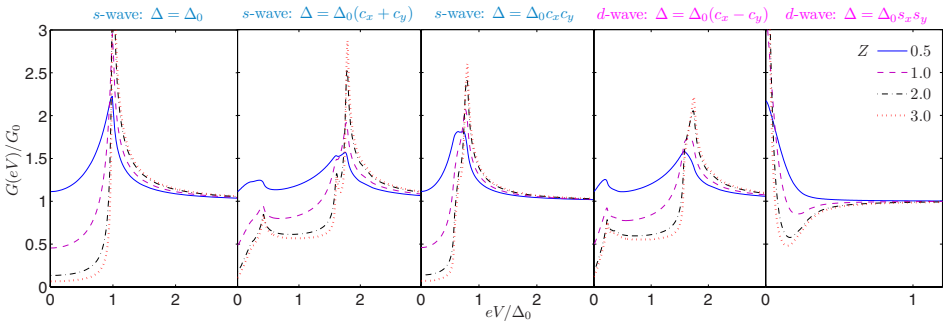

FIG. 2. (Color online) Plot of the conductance spectra for tunneling along the (100) axis in an iron-pnicitide N|S junction for several possible order-parameter symmetries. Only in the d_{xy}-wave case $\Delta=\Delta_0 s_x s_y$ is there a considerable ZBCP. Note the different scale on the voltage axis for this case due to the narrowness of the ZBCP. High (low) values of the parameter Z denote low (high) transmissivity interfaces.

The strategy is now to sum the conductance over the allowed values $k_y \in [-\pi/a, \pi/a]$ for the electronlike ($\lambda=1$) and holelike ($\lambda=-1$) Fermi surfaces and solve for k_x from Eq. (2) by $\Omega_{\mathbf{k}}^{\lambda}=0$ for a given k_y. In what follows, we choose an equal value for the barrier transparencies $Z^+=Z^-\equiv Z$ and gap magnitudes $\Delta_0^+=\Delta_0^-\equiv\Delta_0$ in the two bands for simplicity and add a small imaginary number δ to the quasiparticle energy to model inelastic scattering $eV\rightarrow eV+i\delta$, where $\delta/\Delta_0=10^{-2}$.

As in Ref. 18, we choose $\Delta_0=0.1$. Clearly, it is possible to study a rich variety of interplays between the two quasiparticle bands in terms of different symmetries for the d_{xz} and d_{yz} orbitals and with different gap magnitudes. Here, however, our main aim is to investigate how the conductance spectra are influenced by the nontrivial Fermi-surface topology and dispersion relations and see how this compares with the cylindrical/spherical Fermi surface and free-particle dispersion scenario employed in the usual BTK paradigm. In particular, this is relevant to the interpretation of the point-contact spectroscopy measurements of Refs. 10 and 11. There is, however, an important caveat with regard to which conclusion one may draw with regard to the symmetry of the superconducting OP from the tunneling data of Refs. 10 and 11. In these works, polycrystalline samples were used, while the orbital/nodal structure of the OP can only be convincingly probed in single-crystal specimens. This is because tunneling into polycrystalline samples may lead to intrinsic averaging effects which distort the contribution from anisotropic OPs.

In Fig. 2, we plot the conductance for tunneling along the (100) direction for several OP symmetries. As seen, the d_{xy}-wave case stands out from the rest as it features a considerable ZBCP. Comparing with the experimental data of Ref. 11, we would conclude that a nodal d-wave OP is likely to be realized in $LaFeAsO_{0.9}F_{0.1-\delta}$. The results of Ref. 10 seem to be most consistent with either s-wave or extended s-wave pairing, as only one gap is seen in the spectra. For the s-wave and d_{xy}-wave cases, the standard BTK approach appears to suffice in order to qualitatively say something about the OP symmetry. However, the results are quite different from the usual BTK approach when considering the extended s-wave and $d_{x^2-y^2}$-wave symmetries. More specifically, we find satellite features at subgap energies, including sharp peaks. These features most likely pertain to the specific band structure which we consider here (see Fig. 1) and are thus not possible to capture within the conventional BTK treatment with the cylindrical Fermi-surface approximation. In fact, the density of states (DOS) in our minimal two-band model is a highly nonmonotonic function of energy and contains two Van Hove singularities.[8,17]

Let us also consider the case where there is one fully gapped OP and one nodal OP to see what fingerprints this combination leaves in the conductance spectra. In Fig. 3, we plot the conductance for the case where $\Delta_{\mathbf{k}x}$ is fully gapped, while $\Delta_{\mathbf{k}y}$ has a nodal symmetry. For concreteness, we consider s-wave+d_{xy}-wave pairing and $d_{x^2-y^2}$-wave+d_{xy}-wave pairing in Figs. 3(a) and 3(b), respectively. As seen, the nodal OP gives rise to a ZBCP while there are several satellite features in addition to the large coherence peak at the gap edge. The plots are qualitatively similar regardless of whether the fully gapped OP is s wave or $d_{x^2-y^2}$ wave, while the features in the conductance are qualitatively more pronounced in the s-wave case due to the better gapping of the Fermi surface. Finally, we consider the evolution of the con-

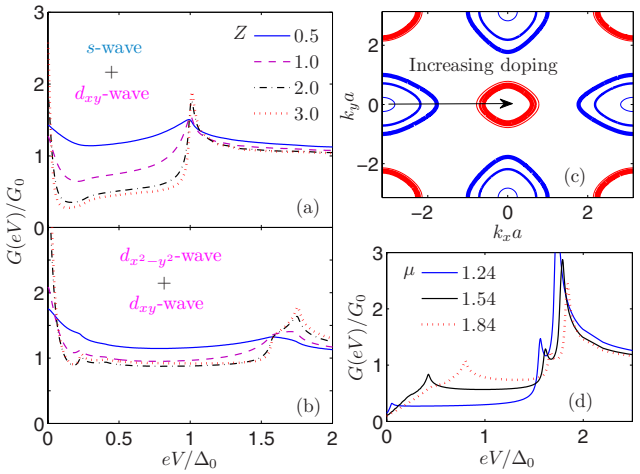

FIG. 3. (Color online) [(a) and (b)] Plot of the conductance spectra for tunneling along the (100) axis in an iron-pnicitide N|S junction for the case of one fully gapped OP and one nodal OP. (c) Evolution of the Fermi-surface topology for $\mu=\{1.24, 1.54, 1.84\}$ in the direction of the arrow. (d) Conductance spectra for the c_x+c_y symmetry with $Z=3$ for different doping levels.

ductance spectra upon changing the doping level μ. The Fermi-surface topology evolves with a change in μ as shown in Fig. 3(c); the electron pockets increase in size while the hole pockets decrease in size upon increasing μ. To see how the subgap features obtained in Fig. 2 evolve upon modifying μ, consider Fig. 3(d) where we provide results for the c_x+c_y symmetry with $Z=3$. As seen, the satellite features shown in Fig. 2 are still present and qualitatively the same, but they are shifted to different bias voltages.

IV. SUMMARY

In summary, we have developed a theory for Andreev reflection in the iron-based high-T_c superconductors. Starting with a tight-binding model on a square lattice to model the puckered FeAs planes, we have investigated several OP symmetries and the resulting conductance spectra. Fully taking into account the Fermi-surface topology and the quasiparticle dispersion relation, we have investigated scenarios where the symmetry of the superconducting OP in both bands is the same and where it is different, i.e., one is fully gapped and the other is nodal. We find that the standard BTK formalism should give qualitatively correct results for the case where the OP symmetries on both bands are either isotropic s wave or d wave. However, the results differ considerably for the extended s-wave symmetries, as we find satellite features at subgap energies which are absent within the usual BTK treatment. Our results may be useful in the context of analyzing quantum transport data of tunneling in normal|superconductor junctions involving the iron pnicitides.

ACKNOWLEDGMENTS

T. Yokoyama is thanked for useful discussions. J.L. and A.S. were supported by the Research Council of Norway under Grants No. 158518/431, No. 158547/431 (NANOMAT), and No. 167498/V30 (STORFORSK).

[1] Y. Kamihara, T. Watanabe, M. Hirano, and H. Hosono, J. Am. Chem. Soc. **130**, 3296 (2008).
[2] H. H. Wen, G. Mu, L. Fang, H. Yang, and X. Y. Zhu, Europhys. Lett. **82**, 17009 (2008).
[3] X. H. Chen, T. Wu, G. Wu, R. H. Liu, H. Chen, and D. F. Fang, Nature (London) **453**, 761 (2008).
[4] Z. A. Ren, J. Yang, W. Lu, W. Yi, G.-C. Che, X.-L. Dong, L.-L. Sun, and Z.-X. Zhao, Mater. Res. Innovations **12**, 105, (2008); Z. A. Ren, G.-C. Che, X.-L. Dong, J. Yang, W. Lu, W. Yi, X.-L. Shen, Z.-C. Li, L.-L. Sun, F. Zhou, and Z.-X. Zhao, Europhys. Lett. **83**, 17002 (2008).
[5] I. I. Mazin, D. J. Singh, M. D. Johannes, and M. H. Du, Phys. Rev. Lett. **101**, 057003 (2008).
[6] R. H. Liu, G. Wu, T. Wu, D. F. Fang, H. Chen, S. Y. Li, K. Liu, Y. L. Xie, X. F. Wang, R. L. Yang, L. Ding, C. He, D. L. Feng, and X. H. Chen, Phys. Rev. Lett. **101**, 087001 (2008).
[7] V. Cvetkovic and Z. Tesanovic, arXiv:0804.4678 (unpublished).
[8] S. Raghu, X.-L. Qi, C.-X. Liu, D. J. Scalapino, and S.-C. Zhang, Phys. Rev. B **77**, 220503(R) (2008).
[9] A. J. Drew, F. L. Pratt, T. Lancaster, S. J. Blundell, P. J. Baker, R. H. Liu, G. Wu, X. H. Chen, I. Watanabe, V. K. Malik, A. Dubroka, K. W. Kim, M. Rössle, and C. Bernhard, Phys. Rev. Lett. **101**, 097010 (2008).
[10] T. Y. Chen, Z. Tesanovic, R. H. Liu, X. H. Chen, and C. L. Chien, Nature (London) **453**, 1224 (2008).
[11] L. Shan, Y. Wang, X. Zhu, G. Mu, L. Fang, C. Ren, and H.-H. Wen, Europhys. Lett. **83**, 57004 (2008).
[12] V. Stanev, J. Kang, and Z. Tesanovic, Phys. Rev. B **78**, 184509 (2008).
[13] G. Deutscher, Rev. Mod. Phys. **77**, 109 (2005).
[14] C.-R. Hu, Phys. Rev. Lett. **72**, 1526 (1994); J. Yang and C.-R. Hu, Phys. Rev. B **50**, 16766 (1994).
[15] G. E. Blonder, M. Tinkham, and T. M. Klapwijk, Phys. Rev. B **25**, 4515 (1982).
[16] Y. Tanaka and S. Kashiwaya, Phys. Rev. Lett. **74**, 3451 (1995); S. Kashiwaya, Y. Tanaka, M. Koyanagi, and K. Kajimura, Phys. Rev. B **53**, 2667 (1996).
[17] G. Xu, W. Ming, Y. Yao, X. Dai, S. Zhang, and Z. Fang, Europhys. Lett. **82**, 67002 (2008).
[18] M. M. Parish, J. Hu, and B. A. Bernevig, Phys. Rev. B **78**, 144514 (2008).
[19] K. Seo, B. A. Bernevig, and J. Hu, Phys. Rev. Lett. **101**, 206404 (2008).